Distribution of deep-water scleractinian and stylasterid corals across abiotic environmental gradients on three seamounts in the Anegada Passage

Steven R. Auscavitch[1], Jay J. Lunden[1], Alexandria Barkman[1], Andrea M. Quattrini[2], Amanda W. J. Demopoulos[3], Erik E. Cordes[1]

[1] Department of Biology, Temple University, Philadelphia, PA, USA.
[2] National Museum of Natural History, Smithsonian Institution, Washington, DC. USA.
[3] Wetland and Aquatic Research Center, U.S. Geological Survey, Gainesville, FL, USA.

Corresponding Author:
Steven R. Auscavitch[1]
steven.auscavitch@temple.edu
1900 N 12th St. Philadelphia, PA, 19122, USA.

Abstract

In the Caribbean Basin, the distribution and diversity patterns of deep-sea scleractinian corals and stylasterid hydrocorals are poorly known compared to their shallow water relatives. In this study, we examined species distribution and community assembly patterns of scleractinian and stylasterid corals on three high-profile seamounts within the Anegada Passage, a deep-water throughway linking the Caribbean Sea and western North Atlantic. Using remotely operated vehicle surveys conducted on the E/V *Nautilus* by the ROV *Hercules* in 2014, we characterized coral assemblages and seawater environmental variables between 162-2157 m on Dog Seamount, Conrad Seamount, and Noroît Seamount. In all, 13 morphospecies of scleractinian and stylasterid corals were identified from video with stylasterids being numerically more abundant than both colonial and solitary scleractinians. Cosmopolitan framework-forming species including *Madrepora oculata* and *Solenosmilia variabilis* were present but occurred in patchy

32   distributions among the three seamounts. Framework-forming species occurred at or above the

33   depth of the aragonite saturation horizon with stylasterid hydrocorals being the only coral taxon

34   observed below Ω_{arag} values of 1. Coral assemblage variation was found to be strongly associated

35   with depth and aragonite saturation state, while other environmental variables exerted less

36   influence. This study enhances our understanding of the factors that regulate scleractinian and

37   stylasterid coral distribution in an underreported marginal sea and establishes a baseline for

38   monitoring future environmental changes due to ocean acidification and deoxygenation in the

39   tropical western Atlantic.

Introduction

42   Global and regional modelling efforts in parallel with observational studies have

43   contributed to our understanding of the distribution of framework-forming azooxanthellate corals

44   in the deep sea (>200 m depth). However, a significant number of data deficient localities persist,

45   most often hindered by a lack of records from direct seafloor observation and *in situ*

46   environmental data. A number of environmental variables have been observed to control the

47   distribution of deep-water azooxanthellate scleractinian corals and stylasterid hydrocorals,

48   including parameters linked to depth, terrain, hydrography, and seawater chemistry (Guinotte et

49   al., 2006; Cairns, 2007; Davies & Guinotte, 2011). In the tropical western Atlantic, a center for

50   deep-water scleractinian diversity (Cairns, 2007), additional direct observational data are needed

51   to validate modelling efforts.

52   The growth of a scleractinian coral colony and formation of the aragonitic calcium

53   carbonate skeleton are generally dependent upon the ambient seawater aragonite saturation state

54   (Ω_{arag}) being greater than 1, or supersaturated. However, some deep-water scleractinian corals,

55   including the cosmopolitan species *Solenosmilia variabilis* and *Enallopsammia rostrata*, have

56   been reported well below the saturation horizon (the depth at which $\Omega_{arag} = 1$) on the Tasmanian

57   Seamounts (Thresher et al., 2011). A more recent survey of seamounts in the Northwestern

58   Hawaiian Islands and Emperor Seamounts documented living colonial scleractinian reefs at Ω_{arag}

59   as low as 0.71 (Baco et al., 2017). Previous studies lend support for targeted observational

60   surveys in underexplored regions in order to delineate species distribution patterns with respect

61   to aragonite saturation and other environmental variables. These efforts are particularly salient in

62   light of potential and ongoing anthropogenic impacts to deep-sea coral ecosystems (Ragnarsson

63   et al., 2017), including global climate change and ocean acidification (Gleckler et al., 2016;

64   Pérez et al., 2018), deep-water drilling and resource extraction (Cordes et al., 2016), bottom-

65   contact fishing (Watling & Norse, 1998), and deep-sea crust mining (Miller et al., 2018).

66   The Greater-Lesser Antilles transition zone is one of the most sparsely surveyed yet

67   biogeographically important deep-water entries from the western Atlantic Ocean into the

68   Caribbean Basin. Topographic features, such as seamounts and other submarine banks associated

69   with deformation along tectonic plate boundaries, are important contributors to the

70   environmental complexity of the deep-sea benthos. In the Anegada Passage, Dog Seamount,

71   Conrad Seamount, Noroît Seamount, and Barracuda Bank are some of the most prominent of the

72   large (> 2 km in height above the surrounding seafloor) seamounts and banks present, ranging

73   from abyssal to mesophotic depths. Typical environmental characteristics of seamounts,

74   including substrate heterogeneity, enhanced productivity and carbon flux, and variable currents

75   (Rogers, 2018), create the potential for deep-water biodiversity hotspots in the region and

76   elevated species abundance relative to the adjacent continental margins and slopes. Previous

77   studies indicate that at depths > 200 m, azooxanthellate corals generally prefer hard substrata that

78   exhibit topographic complexity (Roberts et al., 2009; Georgian, Shedd & Cordes, 2014). As

79   such, seamounts are one example of topographically complex deep-water features that provide

80   ideal hard substrate for corals (Rogers, 1994). Yet very few seamount benthic communities in the

81   Caribbean region have been characterized with respect to these important abiotic gradients.

82   Throughout the tropical western Atlantic, scleractinian species diversity and distributions

83   are relatively well-known from shallow waters but the extent of their distribution below 150 m is

84   poorly understood. For deep-water azooxanthellate corals, 81 species have been reported at

85   depths greater than 50 m for the Greater and Lesser Antilles (Cairns, 2007). As with

86   scleractinians, stylasterid hydrocorals are reportedly diverse from the Lesser Antilles (Cairns,

87   1986), can occur in high densities in the tropical western Atlantic (Messing, Neumann & Lang,

88   1990), and are composed of rigid, primarily aragonitic coralla (Cairns & Macintyre, 1992).

89   Additionally, three-dimensional structures produced by deep-water stylasterids provide habitat

90   for fishes (Love, Lenarz & Snook, 2010) and invertebrate fauna (Braga-Henriques et al., 2011;

91   Reed et al., 2013). Efforts have also been made to understand the biogeographic context of

92   Caribbean ecoregions using deep-water corals in order to support conservation strategies (Cairns

93   & Chapman, 2001; Miloslavich et al., 2010; Hernández-Ávila, 2014). In the Caribbean Basin,

94   patterns in deep-sea coral beta diversity (e.g., species turnover) between ecoregions have been

95   attributed to topography and oceanography (Hernández-Ávila, 2014). Within the insular

96   Caribbean, the Greater Antilles and Lesser Antilles regions are found to diverge into two

97   ecoregions, one encompassing the Greater Antilles islands and the other the Lesser Antilles

98   islands, at continental slope depths (200-2000 m) (Hernández-Ávila, 2014). At larger

99   biogeographic scales and evolutionary time, deep-water currents or water masses have been

100 hypothesized as distribution pathways for constraining cosmopolitan habitat-forming corals like

101   *Lophelia pertusa* in the western Atlantic (Arantes et al., 2009; Henry, 2011). While widespread

102   seamount surveys from the Caribbean Basin remain rare, the effect of environmental variables

103   like temperature, dissolved oxygen, and water mass has been demonstrated for demersal fishes

104   on seamounts in the Anegada Passage (Quattrini et al., 2017).

105   The present study focuses on describing patterns in the distribution of deep-water

106   scleractinians and stylasterid corals on three prominent seamounts in the northeastern Caribbean

107   Sea. In addition to the primary abiotic oceanographic variables including temperature, salinity,

108   and dissolved oxygen, we explore the distribution of aragonitic corals in the region with respect

109   to the aragonite saturation state in this region of the western Atlantic Ocean. As a suspected

110   driver of change in deep-water coral community structure, we also examine the relationship

111   between water mass structure and community similarity in the bathyal zone, hypothesizing that

112   different water masses would have distinct coral assemblages. Finally, we aim to identify abiotic

113   oceanographic variables that most strongly influence the presence of hard corals and their

114   contribution to changes in community similarity for this locality.

115

116   **Materials & Methods**

117

118   *ROV Surveys*

119   This study examined sites within the Anegada Passage in the northeastern corner of the

120   Caribbean Sea (Fig. 1). Three seamounts of varying summit depths were surveyed in September

121   2014 using the ROV *Hercules* during E/V *Nautilus* cruise NA052 (Table 1). Three dives were

122   conducted on Dog Seamount (276 to 1035 m depth), two were conducted on Conrad Seamount

123   (162 to 1314 m depth), and two were conducted on Noroît Seamount (949 to 2206 m depth).

124 Efforts were made to cover similar depth ranges on each feature for direct comparison as

125 permitted by the bathymetry.

126   The ROV was deployed to a maximum target depth on each seamount and generally

127 moved to shallower depths up slope. The ROV continuously traversed the seafloor as near to the

128 bottom as practical at a slow, steady speed (~0.1-0.2 knots, ~0.1 m/s); however, transects were

129 occasionally interrupted by stopping the ROV for sampling and detailed camera zooms. The

130 ROV was equipped with a high-definition camera and paired scaling lasers (10 cm apart). During

131 the dives, the forward-facing cameras were set on wide-angle view, but frequent snap-zooms (up

132 to 20 sec) were conducted to aid in species identification. The ROV was also equipped with a

133 Seabird FastCAT 49 conductivity-temperature-depth (CTD) logger and an Aanderaa oxygen

134 optode to measure dissolved oxygen (DO). The ROV was tracked on the seafloor using an ultra-

135 short baseline (USBL) tracking system as well as a Doppler Velocity Log (DVLNAV).

136

137 *Seawater Collection and Carbonate Chemistry Analysis*

138   Seawater samples ($n = 34$) were collected both in the water column and at the benthos

139 using Niskin bottles mounted to the ROV *Hercules* (Supplementary Table 1). On bottom,

140 seawater samples were collected within 1-2 meters of the benthos and usually co-occurred with

141 the observation of scleractinian colonies on the seafloor. For all seawater samples, co-located

142 physical data (pressure, temperature, salinity, and oxygen) were obtained using vehicle mounted

143 conductivity-temperature-depth (Paroscientific Digiquartz, SBE 49Plus) and oxygen (Aanderaa

144 Optode 3830) sensors, respectively. Upon recovery of the ROV, samples were immediately

145 transferred to 500 mL high-density polyethylene (HDPE) containers according to Best Practices

146 for Ocean CO_2 measurements (Dickson, Sabine & Christian, 2007). While HDPE containers are

147   suitable for long-term storage of seawater for total alkalinity analyses (Huang, Wang & Cai,

148   2012), they are not suitable for long-term storage for pH or dissolved inorganic carbon analyses

149   as they are permeable to CO_2. Accordingly, pH was measured within 1 hour of collection

150   onboard the vessel. Immediately following pH measurement, samples were poisoned with 100

151   µL saturated mercuric chloride solution and stored in a cool, dark location. Total alkalinity was

152   measured in the laboratory in triplicate according to methods previously described (Lunden,

153   Georgian & Cordes, 2013; Georgian et al., 2016a), and final Ω_{arag} values were computed using

154   CO2calc (Robbins et al., 2010). Due to the logistical challenge of pairing a discrete water sample

155   with each individual scleractinian coral observation, we generated a predictive model to

156   interpolate Ω_{arag} at the depth of each coral observation based on temperature, dissolved oxygen,

157   and salinity (for methodology see Georgian et al., 2016a).

158

159   *ROV video analysis*

160   Colonial and solitary coral occurrences were documented using high-definition video

161   transects during each of the ROV dives. Video segments where collections occurred, where the

162   vehicle was too high off the bottom, moving backwards, or of generally poor quality, were

163   removed from analysis. For the purpose of this analysis, we defined structure-forming corals as

164   colonial members of the Scleractinia and hydrozoan family Stylasteridae. Consistent

165   morphospecies identifications were used throughout the analyses. Voucher specimens for

166   morphological identification were obtained using the ROV platform. If necessary, further

167   identifications of coral species were made using taxonomic keys and assistance from taxonomic

168   specialists. Colony height was measured, where possible, by referencing scaling lasers.

169   Individuals or colonies above a 5-cm height threshold were typically identifiable based on laser

170   scalers. If occurrences could not be readily identified below the 5-cm threshold, they were

171   omitted from analysis. Each observation was paired with an associated time-stamp for reference

172   to *in situ* environmental data (temperature, depth, dissolved oxygen concentration, and salinity)

173   collected by ROV CTD and oxygen optode sensors.

174
175   *Community Analyses*
176
177   Sampling effort was evaluated for seamounts individually and for all seamounts combined by

178   sample-based species accumulation curves. In order to assess community relationships among

179   hard-coral assemblages, species abundance values (number of colonies or individuals for each

180   species) were binned into 100 m depth segments for each seamount transect resulting in 28 total

181   samples. Community-level analyses were conducted using standardized and 4th root transformed

182   species abundance data in PRIMER v7 with PERMANOVA add-on (Clarke & Gorley, 2006;

183   Anderson, Gorley & Clarke, 2008). Transformed and standardized species abundances were

184   compiled into a Bray-Curtis resemblance matrix for further analyses. In order to test for

185   significant differences among hard coral assemblages on different seamounts, a one-way analysis

186   of similarity (ANOSIM) was conducted between features as well as between local water masses.

187   Non-metric multidimensional scaling ordinations (nMDS) were conducted across all 28 samples.

188   nMDS plots were overlaid with similarity profile (SIMPROF) analysis to show significant

189   groupings of samples at the 95% level or greater (Clarke, Somerfield & Gorley, 2008). Similarity

190   percentage (SIMPER) tests were used to identify taxa that contributed disproportionately to

191   assemblage similarities within and between seamounts and water masses.

192   Multivariate analyses were also used to explore the abiotic variables relevant to the variation

193   observed in the coral assemblages. Environmental data for temperature, salinity, dissolved

194   oxygen, and Ω_{arag} were obtained from the calculated mean in each 100 m depth segment within

195 every transect. The mean was then 4th-root transformed and normalized within each variable. The

196 BEST (BIO-ENV) routine (Clarke, Somerfield & Gorley, 2008) was applied to the dataset to

197 determine which environmental variables would be useful predictor variables. A distance-based

198 linear model (DistLM) with Akaike information criterion (AIC) was applied using the

199 PERMANOVA add-on in PRIMER v7 (Anderson, Gorley & Clarke, 2008). Visualizations of the

200 resemblance matrix with predictor variables were observed using a dbRDA (distance-based

201 redundancy analysis) ordination with DistLM overlay.

202
203

204 **Results**
205

206 *Survey Summaries*

207 A total of 106 hours of bottom time was assessed across 7 dives (Table 1). Video records

208 were annotated between the depth range of 162-2157 m. In all, 264 observations of solitary and

209 framework-forming scleractinian corals and stylasterid hydrocorals were made across all three

210 seamounts (Table 2). Three dives at Dog Seamount yielded 64 records from 284-849 m. From

211 Conrad Seamount, 182 records were made from 166 m to 1230 m across 2 dives. The deepest

212 two dives at Noroît Seamount had 18 records reported from 1014-1626 m. Stylasterids made up

213 the majority (53%) of coral observations, however most were observed at depths shallower than

214 400 m (Table 2). The majority of scleractinians observed were colonial, framework-forming

215 species (100 colonies observed) while only 22 observations were made of solitary coral species,

216 as they were often on or below the threshold for identification. For this reason, abundances of

217 solitary scleractinians represent a minimum value. No scleractinians or stylasterids above the 5

218 cm size threshold were observed deeper than 1626 m on any seamount.

219

220 *Water Mass Structure*

221

222   Downcast CTD profiles from the ROV sensors were plotted and assessed at each seamount

223 using Ocean Data View v5 (Schlitzer, 2019). Profiles for each seamount were combined to create

224 one consensus profile for the Anegada Passage (Fig. 2). Water masses were identified following

225 published records of temperature, salinity, and dissolved oxygen profiles for the northeast

226 Caribbean and Anegada Passage; these include Subtropical Underwater (SUW) 100-200 m,

227 Sargasso Sea Water (SSW) 200-400 m, Tropical Atlantic Central Water (TACW) 400-700 m,

228 Antarctic Intermediate Water (AAIW) 700-1200 m, and North Atlantic Deep Water (NADW)

229 (>1200 m) (Morrison & Nowlin, 1982).

230

231 *Carbonate chemistry analysis*

232   Water samples for carbonate chemistry analyses were collected at depth from 50 m to

233 2170 m. Total alkalinity ranged from 2291.4 to 2405.9 $\mu mol \cdot kg^{-1}$, and pH ranged from 7.83 to

234 8.11, with minimum pH observed at 795 m depth. Measured Ω_{arag} values from Niskin bottle

235 collections ranged from 4.13 at 50 m depth to 0.99 at 2170 m depth. The aragonite saturation

236 state of the water column was modelled according to the following equation: $\Omega_{arag} = (T \times$

237 $0.11407018) + (O \times 0.00302922) + (S \times 0.18168448) - 6.5216044$ (stepwise backward

238 regression, $R^2 = 0.9857$, $p < 0.001$) where $T =$ temperature in °C, $O =$ oxygen concentration in

239 $\mu mol \cdot L^{-1}$, and $S =$ salinity in parts per thousand (ppt). From this, predicted Ω_{arag} values ranged

240 from 4.11 to 1.05, with highest value at 51 m at Dog Seamount and lowest value at 2195 m at

241 Noroît Seamount.

242

243 *Coral species Distribution Patterns*

244   The single most abundant scleractinian coral species was *Solenosmilia variabilis* (44

245   colonies), but it was only observed on Conrad Seamount in a relatively narrow depth range, 409-

246   569 m. Many structure-forming colonies were found to be associated with boulder and low,

247   outcropping, hard rock substrate. This was followed by the more widespread *Madrepora oculata*

248   (22 colonies), which occurred between 784 and 1540 m on all seamounts (Fig. 3). *Madrepora*

249   *oculata*, which displayed two different growth forms from thin and sparsely branching to thick,

250   robust colonies, possessed the widest depth distribution range for any colonial scleractinian

251   coral. The deepest solitary scleractinian coral, *Javania cailleti*, was observed at 1626 m; this

252   occurrence corresponds with one of the lowest measured Ω_{arag} values of 1.01.

253   The upper bathyal depths, shallower than 700 m, contained species with narrower depth

254   distributions than those at lower bathyal depths (>800 m) (Fig. 3). The sub-700 m assemblage

255   was composed of three species of scleractinians (*E. rostrata*, *M. oculata*, and *J. cailleti*) and one

256   stylasterid (*Crypthelia* sp. 1). The shallowest depths, usually coinciding with the seamount

257   summit, were dominated by two species of stylasterids, *Stylaster* sp. 1 and *Stylaster* cf.

258   *duchassaingi*, as well as one azooxanthellate scleractinian, *Madracis myriaster*. On Conrad

259   Seamount, pink and purple coralline algal crusts were observed as deep as 256 m depth and

260   continued to be observed through shallower depths dominated by sponges, stylasterids, and black

261   corals.

262   The majority of stylasterid species were restricted to depths less than 400 m with only

263   *Crypthelia* exhibiting a wider depth distribution (Fig. 3). Only three morphospecies of

264   stylasterids were large enough to be consistently identified during video annotation. Other

265   unidentifiable stylasterids were combined into a fourth group, Stylasteridae spp. and shown for

266   reference. The most abundant species, *Stylaster* sp. 1, was found in a narrow depth range

267   between 166-174 m on the summit of Conrad Seamount.

268

269   *Patterns of Coral Occurrences with Aragonite Saturation State*

270   Measured Ω_{arag} values from water collected adjacent to corals were not significantly

271   different (t-test, N=9, t=-0.23341, p=0.818) compared to what was calculated using the modelled

272   aragonite saturation state data (Supplementary Fig. 1). All paired water samplings adjacent to

273   coral observations occurred at or above the aragonite saturation horizon (Ω_{arag} >1) (Table 3).

274   Multiple water samples for a single species were collected for only *M. oculata*. A full table of all

275   34 Niskin water bottle measurements and matched environmental variables is provided

276   (Supplementary Table 1).

277   Using predicted values derived from CTD and sensor data on temperature, oxygen

278   concentration, and salinity, all scleractinian and stylasterid corals were observed at Ω_{arag} values

279   of 0.99 to 3.45 (Fig. 4). For scleractinians, *Javania cailleti* occurred across the largest aragonite

280   saturation state range, between 1.01 and 1.77. Among the Stylasteridae, *Crypthelia* sp. 1

281   occurred across the greatest range of saturation states from as low as 0.99 up to 2.83. Only three

282   species were observed at or around the aragonite saturation horizon based on predicted saturation

283   state values, *Crypthelia* sp. 1 (Ω_{arag} =0.99), *M. oculata* (Ω_{arag} =1.00) and *J. cailleti* (Ω_{arag}= 1.01).

284

285   *Community Structure Patterns*

286   Species-accumulation curves were evaluated for seamounts individually and in aggregate for

287   all seamounts. Combined, all seamounts (100-1700 m) revealed a more complete sampling effort

288   than among single seamount coral assemblages (Fig. 5). Individually, species accumulation

289   curves for Dog, Conrad, and Noroît seamounts were not asymptotic, and therefore are likely to

290   accumulate additional coral species with increased sampling effort.

291   Analysis of similarity (two-way nested, depth within seamount, Global R=0.122, p=0.05)

292   conducted among seamounts revealed significant differences in coral assemblages between Dog

293   and Noroît Seamounts (R=0.544, p=0.006), but not Conrad and Dog seamounts (R=-0.001,

294   p=0.379) or Conrad and Noroît seamounts (R=0.029, p=0.292) (Supplementary Table 2). A one-

295   way ANOSIM (Global R=0.464, p=0.001) between water masses revealed significant differences

296   in coral assemblages between SSW and TACW (R=0.46, p=0.003), AAIW (R=0.53, p=0.002),

297   and NADW (R=0.60, p=0.008) as well as between TACW and NADW (R= 0.93, p=0.001) and

298   AAIW and NADW (R=0.361, p=0.01) (Supplementary Table 3).

299   Non-metric multi-dimensional ordination with SIMPROF groupings revealed five statistically

300   significant groupings; two shallow assemblages composed of 100 m depth-binned samples from

301   between 100-600 m and 200-400 m, two mid-depth assemblages (500-700 m and 700-1100 m),

302   and one deep assemblage (1100-1600 m) (Fig. 6). Outliers from these groupings occurred in the

303   600-700 m and 1100-1200 m depth bins on Conrad Seamount and between 1300-1400 m on

304   Noroît Seamount. Within SIMPROF groupings, the shallowest depth grouping showed the

305   greatest amount of dissimilarity among samples (a metric of beta diversity) among the three

306   seamounts while the lowest occurred in the deepest group.

307   Dog Seamount exhibited the lowest beta diversity of coral assemblages among all three

308   seamounts and the highest average similarity at 61% (one-way SIMPER analysis), with the

309   average similarity between 100 m depth bins being most strongly influenced by *Crypthelia* sp.

310   1, which contributed to 96.6% of the relative abundance. Noroît Seamount had the second

311   highest similarity (38.2%), with *M*. *oculata* accounting for 84.7% of the similarity. Conrad

312   Seamount had the lowest average similarity (15%), with stylasterids *Crypthelia* sp. 1 and

313   *Stylaster* cf. *duchassaingi* being the greatest contributors to average similarity with 48.4% and

314   21.5%, respectively. Between seamounts, Noroît differed from Dog and Conrad, primarily due to

315   the higher abundance of *M. oculata* at Noroît Seamount. Noroît Seamount had nearly triple the

316   average abundance of *M. oculata* compared to Conrad Seamount. Conrad and Dog Seamounts

317   differed primarily due to the contribution of *Crypthelia* sp. 1 and *M. myriaster*, which were

318   present on Conrad at 2 to 3 times higher average abundance than at Dog Seamount.

319   Within water masses, the greatest average similarity of coral assemblages occurred within

320   NADW (54%) followed by TACW (51%) and finally SSW at (32 %). The abundance of

321   scleractinians was responsible for greater similarities within deep water masses (*M. oculata* and

322   *Javania cailleti* in NADW) while stylasterids were more commonly associated with driving

323   patterns of similarity within intermediate and shallower water masses (*Crypthelia* sp. 1 in

324   TACW, AAIW and *Stylaster* cf. *duchassaingi* in SSW). Between immediately adjacent water

325   masses, the greatest average dissimilarity was observed between SUW and SSW (92.3%) and the

326   lowest between TACW and AAIW (56.7%), indicating higher rates of turnover (beta diversity)

327   for shallower water masses than deeper ones.

328   Results from the BEST analysis indicated that the largest percentage of biological variation

329   was correlated with depth (r=0.536). The BEST routine also indicated that the greatest

330   correlation occurred with the four combined factors of depth, Ω_{arag}, temperature, and dissolved

331   oxygen (r=0.614). Sequential tests in the DistLM analysis indicated that depth (AIC=223.88,

332   p=0.001) and Ω_{arag} (AIC= 215.87, p=0.001) were the greatest explanatory variables influencing

333   coral assemblages on seamounts in the Anegada Passage. Temperature, salinity, and oxygen did

334   not explain a significant portion of the biological variation in this test. Redundancy analyses

335 resulted in 59.4% of the DistLM model variation explained by the primary axis (dbRDA1) and

336 32.6% explained by the second (dbRDA2) (Fig. 7). Likewise, the first axis explained 32.8% of

337 the total biological variation observed and the second axis explained 18%. The primary axis was

338 most closely correlated with oxygen (r = -0.82), while the second was most closely related to

339 temperature (r= -0.61).

340

341

Discussion

343   Seamounts in the Anegada Passage were found to harbor communities of stony and lace

344 corals throughout the bathyal depth range from summit depths as shallow as 166 m to a

345 maximum of 1626 m. Both stylasterid and scleractinian coral species with aragonitic skeletons

346 were largely present above the aragonite saturation horizon in this region of the western Atlantic

347 Ocean, with the understanding that sampling effort below the ASH was limited to one transect at

348 Noroît Seamount (Table 1). Nevertheless, we were able to identify the depth of the ASH as

349 occurring between 2000-2200 m in the Anegada Passage (Supplementary Fig. 1), which is

350 consistent with previous reports from the North Atlantic Ocean (Jiang et al., 2015). Only

351 stylasterids in the genus *Crypthelia* were observed to occur below the aragonite saturation

352 horizon (Ω_{arag} =0.99), but others, including the framework-forming species *Madrepora oculata*,

353 occurred at saturation states as low as Ω_{arag} =1.0. Given the present findings and that aragonitic

354 coral species have been observed at depths below that of the ASH (>2000 m) in other parts of the

355 Caribbean Basin (Cairns 1979), it is still reasonable to expect that aragonitic corals can persist

356 below the aragonite saturation horizon within the Anegada Passage. Also noteworthy was the

357   observation of live crustose coralline algae at a depth of 256 m, which is comparable to the

358   deepest known record from San Salvador Island (268 m) in The Bahamas (Littler et al., 1986).

359   Overlying water masses were a significant indicator of community assembly differences

360   between SSW (Sargasso Sea Water) and deeper water masses, but not the shallowest water mass,

361   Subtropical Underwater (SUW) and deeper strata of the water column. Oceanographic variables

362   that most strongly influenced the presence of aragonitic corals and their contribution to changes

363   in community similarity were depth and aragonite saturation state, with temperature, salinity, and

364   dissolved oxygen making less significant contributions.

365   The tropical western Atlantic is a known diversity center for azooxanthellate scleractinian

366   corals and stylasterid hydrocorals (Cairns, 2007, 2011). This study provides new distribution

367   records for deep-water coral species in the northeastern Caribbean and builds on existing efforts

368   to characterize the azooxanthellate coral fauna of the tropical western Atlantic (Cairns, 1979;

369   Cairns & Chapman, 2001; Lutz & Ginsburg, 2007). Specifically, 7 species or morphospecies of

370   stony corals within the genera *Javania*, *Madrepora*, *Madracis*, *Enallopsammia*, *Dendrophyllia*,

371   and *Caryophyllia* have been added to local species inventories in the Anegada Passage (Fig. 8).

372   New records from photographic and physical specimens aid in resolving the complex

373   biogeography of the Greater-Lesser Antilles Transition zone seamounts with respect to the

374   western North Atlantic (Supplementary Table 4). The paucity of records paired with

375   environmental parameters from global biogeographic databases makes these observations critical

376   to understanding the species distribution dynamics of marginal Atlantic seas and how coral

377   distribution may be affected by future ocean climatic changes.

378   Stony coral assemblages in the Anegada Passage were similar to those observed in other

379   parts of the western Atlantic Ocean with a few noteworthy absences. Absent from our records

380   from the Anegada Passage seamounts include reef-forming species like *L. pertusa* and *E.*

381   *profunda*, as well as cosmopolitan cup coral species like *Desmophyllum dianthus*, which are

382   reportedly more common throughout the U.S. southeast continental shelf and Gulf of Mexico

383   (Schroeder et al., 2005; Reed, Weaver & Pomponi, 2006; Brooke & Schroeder, 2007; Lunden,

384   Georgian & Cordes, 2013; Georgian et al., 2016a). While fossilized *Lophelia* rubble have been

385   reported in the Colombian Caribbean (Santodomingo et al., 2007) and live *Lophelia* has been

386   observed on the Brazilian continental margin (Arantes et al., 2009), the southern Caribbean

387   (Hernández-Ávila, 2014), and off Roatan, Honduras (Henry, 2011), members of this genus have

388   not been extensively reported in the insular Caribbean (OBIS, 2019).

389   We were also able to identify some variability in local distribution patterns among

390   seamounts for three colonial scleractinian species. *Enallopsammia rostrata*, *Dendrophyllia*

391   *alternata*, and *Solenosmilia variabilis* appear to have patchy distributions on the Anegada

392   Passage seamounts. For example, only two colonies of *E. rostrata* were observed, both on Dog

393   Seamount at 785m, and only five colonies of *D. alternata* were observed on Conrad Seamount

394   between 490-598 m (Fig. 3). Similarly, *S. variabilis* was only observed in patches on Conrad

395   Seamount from 490-569 m (Fig. 3). S*olenosmilia* has not been widely reported from the greater

396   Caribbean basin based on records from the Ocean Biogeographic Information System (OBIS,

397   2019), but is known to be a contributor to coral mound formation off Brazil (Raddatz et al.,

398   2020). *Solenosmilia* has been more commonly reported to asexually reproduce, and thus has a

399   relatively short dispersal ability (Miller & Gunasekera, 2017), potentially explaining its patchy

400   distribution.

401   Several coral taxa encountered in the Anegada Passage are important species for

402   understanding biogeographic patterns of the Caribbean bathyal zone. *Madracis myriaster* was

403 observed both on Dog and Conrad Seamounts, but only between 253 - 311 m. This depth range

404 is also similar to that observed in the western North Atlantic off Bermuda (90-300 m)

405 (Stefanoudis et al. 2019). In the Caribbean, *M. myriaster* has been observed at similar depths and

406 in high densities during surveys by the ROV *Deep Discoverer* on the NOAA Ship *Okeanos*

407 *Explorer* east of Vieques Island and in the Mona Passage (Wagner et al., 2019). Northern and

408 eastern Caribbean coral communities at continental shelf depths have been found to be dissimilar

409 from the southern Caribbean, such that they may constitute distinct ecoregions (Hernández-

410 Ávila, 2014). These differences were found to be driven by differences in the abundance of *M.*

411 *myriaster* (Fig. 8C), which is more common at mesophotic and upper bathyal depths (Reyes et

412 al., 2005; Santodomingo et al., 2007; Hernández-Ávila, 2014; Stefanoudis et al. 2019). At lower

413 bathyal depths, regional biogeographic differences have also been attributed to variation in the

414 frequency of solitary scleractinian species (e.g. *Stephanocyathus* spp., *Fungiacyathus* sp.) that

415 may be difficult to detect during video transects (Hernández-Ávila, 2014). A greater diversity of

416 solitary scleractinian corals and smaller stylasterids may have been present in the video but could

417 not be documented due to limitations of ROV surveys (discussed in Everett & Park, 2018). The

418 lack of easily identifiable diagnostic features from video, rugose terrain (e.g. overhangs and

419 ledges), and rarity make most smaller species difficult to identify from ROV surveys without

420 voucher specimens. A more thorough analysis incorporating modern (e.g. higher-resolution ROV

421 video surveys with *in situ* collections) and historical datasets (e.g. museum-archived specimens)

422 would be helpful in elucidating biogeographic patterns more broadly across the basin.

423   Several species in the genus *Crypthelia* occur in the eastern Caribbean at bathyal depths

424 (Cairns, 1986). The difficulty of identifying stylasterids from ROV video remains a challenge in

425 establishing species occurrences, necessitating a voucher collection to confirm morphospecies

426   identity. Nevertheless, the depth distribution, colony morphology, and coloration of *Stylaster* sp.

427   1, is consistent with *Stylaster roseus* (Pallas, 1766), a tropically-distributed western Atlantic

428   stylasterid from depths typically less than 500 m (OBIS, 2019). *Crypthelia* sp. and other

429   stylasterid species are more likely to be underreported due to their small size (2-5 cm), on the

430   threshold of being able to be accurately recorded from ROV video. These stylasterids were also

431   observed under overhangs which made obtaining an accurate account of their abundance

432   difficult. In this case, the reported occurrences of these corals represent a minimum value.

433   The ecological contribution of stylasterid corals is often understated, despite the ability of

434   some species to produce significant three-dimensional structures that can act as habitat for other

435   organisms. Larger structure-forming stylasterids are functionally analogous to some colonial

436   scleractinian corals in that they can provide habitat for larger organisms such as deep-water

437   fishes and invertebrates (Love, Lenarz & Snook, 2010; Braga-Henriques et al., 2011). *Crypthelia*

438   spp., while relatively abundant in places and occurring over a wide range, were never observed

439   above 12 cm in overall height and were observed to be extremely brittle when attempting

440   collection (Fig. 9A). However, two species in the genus *Stylaster*, *S.* cf. *duchassaingi* (Fig. 9B)

441   and *Stylaster* sp. 1 (Fig. 9C), can be classified as potentially important three-dimensional

442   structure-forming species, primarily occurring between 150- 400 m depth.

443   The carbonate mineralogy of most stylasterids is similar to scleractinians in that a

444   majority of known species, including those observed in this study, produce a skeleton composed

445   primarily of the mineral aragonite (Cairns, 2011), although some are calcitic in composition

446   (Cairns & Macintyre, 1992). Stylasterids do share distribution characteristics and overlapping

447   depth ranges with many upper bathyal solitary and colonial scleractinian corals (Cairns, 1986,

448 2011). Like scleractinians, stylasterid hydrocorals also exhibit a vulnerability to changing

449 aragonite saturation conditions over their depth distribution (Guinotte et al., 2006).

450

451   Knowledge of the chemical environment of deep-sea scleractinians has grown

452 significantly in recent years as empirical measurements of the carbonate system at deep-sea coral

453 habitats have been reported from different regions across the global ocean. On seamounts in the

454 Indian Ocean off the coast of SW Australia, the majority of framework-forming scleractinians –

455 including *E. rostrata* and *S. variabilis* – were found at Ω_{arag} values at or just below saturation,

456 suggesting a control on the lower limit of these species' distributions (Thresher et al., 2011).

457 However, live scleractinian reefs were recently discovered on seamounts in the North Pacific at

458 Ω_{arag} values as low as 0.71 (Baco et al., 2017) and as low as 0.81 off Southern California (Gómez

459 et al., 2018). Additionally, scleractinians have been observed below the ASH in the Indian Ocean

460 (Trotter et al., 2019) and South Atlantic Ocean (Barbosa, Davies & Sumida, 2020). These

461 revelations indicate that, under the right conditions, scleractinian corals can persist in

462 undersaturated waters (Baco et al., 2017). Additionally, the presence of live tissue may buffer

463 against the effects of low pH (Venn et al., 2011), but the underlying dead coral framework may

464 be less resilient to undersaturated waters. Expanded surveys below 2000 m in northern

465 Caribbean, in tandem with additional effort in sampling of coral-adjacent deep-waters for

466 carbonate chemistry analysis will aid in better determining the controls on aragonitic coral

467 species distribution at lower bathyal depths in the tropical western Atlantic.

468   Productivity of the surface waters and export to the deep-sea benthos may contribute to

469 differences in species distribution and abundance of deep-sea corals. In a 2016 laboratory

470 experiment and field study comparing two spatially distinct and genetically isolated populations

471 of the framework-forming scleractinian *Lophelia pertusa*, colonies from Norway exhibited

472 enhanced respiration and prey capture rates under acidified conditions compared to individuals

473 from the Gulf of Mexico (Georgian et al., 2016b). This study lends support to the hypothesis that

474 species are locally adapted to environmental conditions, including food supply, which may allow

475 individuals to better tolerate reduced carbonate saturation states.

476 **Conclusions**

477

478 Our results offer some insights to the distribution, diversity, and drivers of community

479 assembly of scleractinian and stylasterid deep-water corals in a data-deficient region of the

480 tropical western Atlantic Ocean. These findings lend support for the efficacy of targeted

481 exploration surveys to understand coral distribution with respect to environmental gradients in

482 the deep-sea environment. The presence of aragonitic corals, largely occurring above the

483 aragonite saturation horizon, was not unexpected, but more surprising was the presence of

484 known framework-forming scleractinians, like *Madrepora oculata*, living at or just above Ω_{arag}

485 =1 in this locality. Future work should seek to expand upon coral community inventories for this

486 area to include members of the Octocorallia and Antipatharia, particularly to refine the

487 relationship between community assembly and water mass structure. Increased taxonomic effort

488 is needed to better identify cryptic coral morphospecies from the deep-sea benthos, and

489 particularly for those size classes below the identification threshold for ROV video surveys. In

490 the Atlantic Ocean, deep-water coral ecosystem health is likely to be negatively impacted by

491 environmental change by the end of the current century. Warming deep-waters (Gleckler et al.,

492 2016), thermohaline driven deep-water acidification (Pérez et al., 2018), and low latitude

493 deoxygenation in the Atlantic (Montes et al., 2016) are among the greatest threats facing deep-

494 water framework-forming corals. The relationship between coral occurrences and environmental

495   variables reported here establish a critical baseline for the detection of the effects of deep ocean

496   change to seafloor communities, which is crucial to effective conservation.

497

498   **Acknowledgements**

499

500   We would like to thank the efforts of the science party, master, and crew of the E/V *Nautilus*

501   during the *Exploration of the Anegada Passage* (NA052) cruise. In addition, we would like to

502   extend a special thanks to the Ocean Exploration Trust for their support. Taxonomic assistance in

503   identifying voucher material was provided by Stephen Cairns (National Museum of Natural

504   History, Smithsonian Institution) for scleractinian and stylasterid corals. We would also like to

505   thank Jason Chaytor, Alex Rogers, Iván Hernández-Ávila, and Nadia Santodomingo for their

506   feedback in the revision of this manuscript. Any use of trade, firm, or product names is for

507   descriptive purposes only and does not imply endorsement by the U.S. Government.

508

509   **References**

510

511   Anderson M, Gorley RN, Clarke RK. 2008. *Permanova+ for Primer: Guide to Software and*

512   *Statistical Methods*. Primer-E Limited.

513   Arantes RCM, Castro CB, Pires DO, Seoane JCS. 2009. Depth and water mass zonation and

514   species associations of cold-water octocoral and stony coral communities in the

515   southwestern Atlantic. *Marine Ecology Progress Series* 397:71–79. DOI:

516   10.3354/meps08230.

517   Baco AR, Morgan N, Roark EB, Silva M, Shamberger KEF, Miller K. 2017. Defying

518   Dissolution: Discovery of Deep-Sea Scleractinian Coral Reefs in the North Pacific.

519   *Scientific Reports* 7:1–11. DOI: 10.1038/s41598-017-05492-w.

520   Barbosa R V, Davies AJ, Sumida PYG. 2020. Habitat suitability and environmental niche

521   comparison of cold-water coral species along the Brazilian continental margin. *Deep Sea*

522   *Research Part I: Oceanographic Research Papers* 155:103147.

523   Braga-Henriques A, Carreiro-Silva M, Porteiro FM, De Matos V, Sampaio Í, Ocaña O, Ávila SP.

524   2011. The association between a deep-sea gastropod *Pedicularia sicula* (Caenogastropoda:

525   Pediculariidae) and its coral host Errina dabneyi (Hydrozoa: Stylasteridae) in the Azores.

526   *ICES Journal of Marine Science* 68:399–407. DOI: 10.1093/icesjms/fsq066.

527   Brooke S, Schroeder WW. 2007. State of deep coral ecosystems in the Gulf of Mexico region:

528   Texas to the Florida Straits. *The State of Deep Coral Ecosystems of the United States*:271–

529   306.

530   Cairns SD. 1979. The deep-water Scleractinia of the Caribbean Sea and adjacent waters. *Studies*

531   *on the Fauna of Curaçao and other Caribbean Islands* 57:1–341.

532   Cairns SD. 1986. A revision of the northwest Atlantic Stylasteridae (Coelenterata: Hydrozoa).

533   *Smithsonian Contributions to Zoology* 418:1–131. DOI: 10.5479/si.00810282.418.

534   Cairns SD. 2007. Deep-water corals: An overview with special reference to diversity and

535   distribution of deep-water scleractinian corals. *Bulletin of Marine Science* 81:311-322.

536   Cairns SD. 2011. Global Diversity of the Stylasteridae (Cnidaria: Hydrozoa: Athecatae). *PLoS*

537   *ONE* 6:1-13. DOI: 10.1371/journal.pone.0021670.

538   Cairns SD, Chapman RE. 2001. Biogeographic affinities of the North Atlantic deep-water

539   Scleractinia. *Proceedings of the First International Symposium on Deep-Sea Corals 1:30-*

540   *57*.

541   Cairns SD, Macintyre IG. 1992. Phylogenetic implications of calcium carbonate mineralogy in

542   the Stylasteridae (Cnidaria: Hydrozoa). *Palaios 7*:96–107.

543   Clarke KR, Gorley RN. 2006. User manual/tutorial. *PRIMER-E Ltd., Plymouth*.

544   Clarke KR, Somerfield PJ, Gorley RN. 2008. Testing of null hypotheses in exploratory

545   community analyses: similarity profiles and biota-environment linkage. *Journal of*

546   *Experimental Marine Biology and Ecology* 366:56–69. DOI: 10.1016/j.jembe.2008.07.009.

547   Cordes EE, Jones DOB, Schlacher TA, Amon DJ, Bernardino AF, Brooke S, Carney R, DeLeo

548   DM, Dunlop KM, Escobar-Briones EG, Gates AR, Génio L, Gobin J, Henry LA, Herrera S,

549   Hoyt S, Joye M, Kark S, Mestre NC, Metaxas A, Pfeifer S, Sink K, Sweetman AK, Witte U.

550   2016. Environmental impacts of the deep-water oil and gas industry: A review to guide

551   management strategies. *Frontiers in Environmental Science* 4:1-26. DOI:

552   10.3389/fenvs.2016.00058.

553   Davies AJ, Guinotte JM. 2011. Global habitat suitability for framework-forming cold-water

554   corals. *PloS one* 6:e18483.

555   Dickson AG, Sabine CL, Christian JR. 2007. *Guide to best practices for ocean CO2*

556   *measurements*. North Pacific Marine Science Organization.

557   https://www.oceanbestpractices.net/handle/11329/249

558   Everett M V., Park LK. 2018. Exploring deep-water coral communities using environmental

559   DNA. *Deep Sea Research Part II: Topical Studies in Oceanography* 150:229–241. DOI:

560   10.1016/J.DSR2.2017.09.008.

561   Georgian SE, DeLeo D, Durkin A, Gomez CE, Kurman M, Lunden JJ, Cordes EE. 2016a.

562   Oceanographic patterns and carbonate chemistry in the vicinity of cold-water coral reefs in

563   the Gulf of Mexico: Implications for resilience in a changing ocean. *Limnology and*

564   *Oceanography* 61:648–665.

565   Georgian SE, Dupont S, Kurman M, Butler A, Strömberg SM, Larsson AI, Cordes EE. 2016b.

566   Biogeographic variability in the physiological response of the cold-water coral *Lophelia*

567   *pertusa* to ocean acidification. *Marine Ecology* 37:1345–1359. DOI: 10.1111/maec.12373.

568   Georgian SE, Shedd W, Cordes EE. 2014. High-resolution ecological niche modelling of the

569   cold-water coral *Lophelia pertusa* in the Gulf of Mexico. *Marine Ecology Progress Series*

570   506:145–161. DOI: 10.3354/meps10816.

571   Gleckler PJ, Durack PJ, Stouffer RJ, Johnson GC, Forest CE. 2016. Industrial-era global ocean

572   heat uptake doubles in recent decades. *Nature Climate Change* 6:394–398. DOI:

573   10.1038/nclimate2915.

574   Gómez CE, Wickes L, Deegan D, Etnoyer PJ, Cordes EE. 2018. Growth and feeding of deep-sea

575   coral *Lophelia pertusa* from the California margin under simulated ocean acidification

576   conditions. *PeerJ* 6:e5671. DOI: 10.7717/peerj.5671.

577   Guinotte JM, Orr J, Cairns S, Freiwald A, Morgan L, George R. 2006. Will human-induced

578   changes in seawater chemistry alter the distribution of deep-sea scleractinian corals?

579   *Frontiers in Ecology and the Environment* 4:141–146.

580   Henry LA. 2011. A deep-sea coral 'gateway' in the northwestern Caribbean. In: Palomares

581   MLD, Pauly D (eds.), *Too Precious to Drill: the Marine Biodiversity of Belize*. Fisheries

582   Centre Research Reports 19:120-124. Fisheries Centre, University of British Columbia.

583   Hernández-Ávila I. 2014. Patterns of deep-water coral diversity in the Caribbean basin and

584   adjacent southern waters: An approach based on records from the R/V Pillsbury

585   expeditions. *PLoS ONE* 9:1-11. DOI: 10.1371/journal.pone.0092834.

586   Huang W, Wang Y, Cai W. 2012. Assessment of sample storage techniques for total alkalinity

587   and dissolved inorganic carbon in seawater. *Limnology and oceanography: Methods*

588   10:711–717.

589   Jiang L, Feely RA, Carter BR, Greeley DJ, Gledhill DK, Arzayus KM. 2015. Climatological

590   distribution of aragonite saturation state in the global oceans. *Global Biogeochemical*

591   *Cycles* 29:1656–1673. DOI: 10.1002/2015GB005198.

592   Littler MM, Littler DS, Blair SM, Norris JN. 1986. Deep-water plant communities from an

593   uncharted seamount off San Salvador Island, Bahamas: distribution, abundance, and primary

594   productivity. *Deep-sea Research* 33:881–892.

595   Love MS, Lenarz B, Snook L. 2010. A survey of the reef fishes, purple hydrocoral (*Stylaster*

596   *californicus*), and marine debris of Farnsworth Bank, Santa Catalina Island. *Bulletin of*

597   *Marine Science* 86:35–52.

598   Lunden JJ, Georgian SE, Cordes EE. 2013. Aragonite saturation states at cold-water coral reefs

599   structured by *Lophelia pertusa* in the northern Gulf of Mexico. *Limnology and*

600   *Oceanography* 58:354–362. DOI: 10.4319/lo.2013.58.1.0354.

601   Lutz SJ, Ginsburg RN. 2007. State of deep coral ecosystems in the Caribbean region: Puerto

602   Rico and the US Virgin Islands. *The State of Deep Coral Ecosystems of the United States.*

603   *NOAA Technical Memorandum CRCP-3, Silver Spring, MD*:307–365.

604   Messing CG, Neumann AC, Lang JC. 1990. Biozonation of Deep-Water Lithoherms and

605   Associated Hardgrounds in the Northeastern Straits of Florida. *Palaios* 5:15–33.

606   Miller KJ, Gunasekera RM. 2017. A comparison of genetic connectivity in two deep sea corals

607   to examine whether seamounts are isolated islands or stepping stones for dispersal.

608   *Scientific Reports* 7:1–14. DOI: 10.1038/srep46103.

609   Miller KA, Thompson KF, Johnston P, Santillo D. 2018. An overview of seabed mining

610   including the current state of development, environmental impacts, and knowledge gaps.

611   *Frontiers in Marine Science* 4:418. DOI: 10.3389/fmars.2017.00418.

612 Miloslavich P, Díaz JM, Klein E, Alvarado JJ, Díaz C, Gobin J, Escobar-Briones E, Cruz-Motta

613   JJ, Weil E, Cortés J, Bastidas AC, Robertson R, Zapata F, Martín A, Castillo J, Kazandjian

614   A, Ortiz M. 2010. Marine biodiversity in the caribbean: Regional estimates and distribution

615   patterns. *PLoS ONE* 5:1-25. DOI: 10.1371/journal.pone.0011916.

616 Montes E, Muller-karger FE, Cianca A, Lomas MW, Lorenzoni L, Habtes S. 2016. Decadal

617   variability in the oxygen inventory of North Atlantic subtropical underwater captured by

618   sustained, long-term oceanographic time series observations. *Global Biogeochemical Cycles*

619   30:460–478. DOI: 10.1002/2015GB005183.Received.

620 Morrison JM, Nowlin WD. 1982. General distribution of water masses within the eastern

621   Caribbean Sea during the winter of 1972 and fall of 1973. *Journal of Geophysical*

622   *Research: Oceans* 87:4207–4229.

623 OBIS. 2019. Ocean Biogeographic Information System. *Intergovernmental Oceanographic*

624   *Commission of UNESCO.*

625 Pérez FF, Fontela M, Garcia-Ibañez MI, Mercier H, Velo A, Lherminier P, Zunino P, de la Paz

626   M, Alonso-Pérez F, Guallart EF, Padin XA. 2018. Meridional overturning circulation

627   conveys fast acidification to the deep Atlantic Ocean. *Nature*. 554:515-518 DOI:

628   10.1038/nature25493.

629 Quattrini AM, Demopoulos AWJ, Singer R, Roa-Varon A, Chaytor JD. 2017. Demersal fish

630   assemblages on seamounts and other rugged features in the northeastern Caribbean. *Deep*

631   *Sea Research Part I: Oceanographic Research Papers* 123:90-104. DOI:

632   10.1016/j.dsr.2017.03.009.

633 Raddatz J, Titschack J, Frank N, Freiwald A, Conforti A, Osborne A, Skornitzke S, Stiller W,

634   Rüggeberg A, Voigt S, Albuquerque ALS, Vertino A, Schröder-Ritzrau A, Bahr A. 2020.

635   *Solenosmilia variabilis*-bearing cold-water coral mounds off Brazil. *Coral Reefs* 39:69–83.

636   DOI: 10.1007/s00338-019-01882-w.

637 Ragnarsson SÁ, Burgos JM, Kutti T, Beld I Van Den, Egilsdóttir H, Arnaud-haond S, Grehan A.

638   2017. The impact of Anthropogenic Activity on Cold-Water Corals. In: Rossi S ed. *Marine*

639   *Animal Forests*. Springer International Publishing, 1–35. DOI: 10.1007/978-3-319-17001-5.

640 Reed JK, Messing C, Walker BK, Brooke S, Correa TBS, Brouwer M, Udouj T, Farrington S.

641   2013. Habitat characterization, distribution, and areal extent of deep-sea coral ecosystems

642   off Florida, southeastern U.S.A. *Caribbean Journal of Science* 47:13–30. DOI:

643   10.18475/cjos.v47i1.a3.

644 Reed JK, Weaver DC, Pomponi SA. 2006. Habitat and fauna of deep-water *Lophelia pertusa*

645   coral reefs off the southeastern US: Blake Plateau, Straits of Florida, and Gulf of Mexico.

646   *Bulletin of Marine Science* 78:343–375.

647 Reyes J, Santodomingo N, Gracia A, Borrero-Pérez G, Navas G, Mejía-Ladino LM, Bermúdez

648   A, Benavides M. 2005. Southern Caribbean azooxanthellate coral communities off

649   Colombia. In: *Cold-water corals and Ecosystems*. Springer, 309–330.

650 Robbins LL, Hansen ME, Kleypas JA, Meylan SC. 2010. *CO2calc: A user-friendly seawater*

651   *carbon calculator for Windows, Mac OS X, and iOS (iPhone)*. US Geological Survey.

652 Roberts JM, Wheeler A, Freiwald A, Cairns SD. 2009. *Cold-water corals: the biology and*

653   *geology of deep-sea coral habitats*. Cambridge University Press, 1-334.

654 Rogers AD. 1994. The biology of seamounts. In: *Advances in marine biology*. Elsevier, 305–

655   350.

656 Rogers AD. 2018. The Biology of Seamounts: 25 Years on. *Advances in Marine Biology*

657   79:137–224. DOI: 10.1016/BS.AMB.2018.06.001.

658   Santodomingo N, Reyes J, Gracia A, Martínez A, Ojeda G, García C. 2007. Azooxanthellate

659   Madracis coral communities off San Bernardo and Rosario Islands (Colombian Caribbean).

660   *Bulletin of Marine Science* 81:273–287.

661   Schlitzer R. 2019. Ocean data view. Available at: https://odv.awi.de/

662   Schroeder WW, Brooke SD, Olson JB, Phaneuf B, McDonough JJ, Etnoyer P. 2005. Occurrence

663   of deep-water *Lophelia pertusa* and *Madrepora oculata* in the Gulf of Mexico. In: *Cold-*

664   *water corals and ecosystems*. Springer, 297–307.

665   Stefanoudis P V., Rivers M, Smith SR, Schneider CW, Wagner D, Ford H, Rogers AD, Woodall

666   LC. 2019. Low connectivity between shallow, mesophotic and rariphotic zone benthos.

667   *Royal Society Open Science* 6:1-13. DOI: 10.1098/rsos.190958.

668   Thresher RE, Tilbrook B, Fallon S, Wilson NC, Adkins J. 2011. Effects of chronic low carbonate

669   saturation levels on the distribution, growth and skeletal chemistry of deep-sea corals and

670   other seamount megabenthos. *Marine Ecology Progress Series* 442:87–99. DOI:

671   10.3354/meps09400.

672   Trotter JA, Pattiaratchi C, Montagna P, Taviani M, Falter J, Thresher R, Hosie A, Haig D,

673   Foglini F, Hua Q. 2019. First ROV exploration of the Perth Canyon: Canyon setting, faunal

674   observations, and anthropogenic impacts. *Frontiers in Marine Science 6:1-24*.

675   Venn A, Tambutté E, Holcomb M, Allemand D, Tambutté S. 2011. Live tissue imaging shows

676   reef corals elevate pH under their calcifying tissue relative to seawater. *PLoS ONE* 6:1-9.

677   DOI: 10.1371/journal.pone.0020013.

678   Wagner D, Sowers D, Williams SM, Auscavitch S, Blaney D, Cromwell M. 2019. *Océano*

679   *Profundo 2018: Exploring deep sea habitats off Puerto Rico and the US Virgin Islands*.

680   Office of Ocean Exploration and Research, NOAA, Silver Spring, MD 20910, OER

681   Expedition Report EX-18-11, 1-171. DOI: 10.25923/wc2n-qg29

682   Watling L, Norse EA. 1998. Disturbance of the Seabed by Mobile Fishing Gear: A Comparison

683   to Forest Clearcutting. *Conservation Biology* 12:1180–1197.

684

685
686

Figure 1

Multibeam bathymetric map of the Anegada Passage seamounts.

The locations of Dog, Conrad, and Noroît Seamount are indicated in bold. Dive locations are overlaid in yellow and labeled by dive number. The bathymetry color ramp in the lower right indicates depth values measured in meters. Transect segments lengths are not drawn to scale.
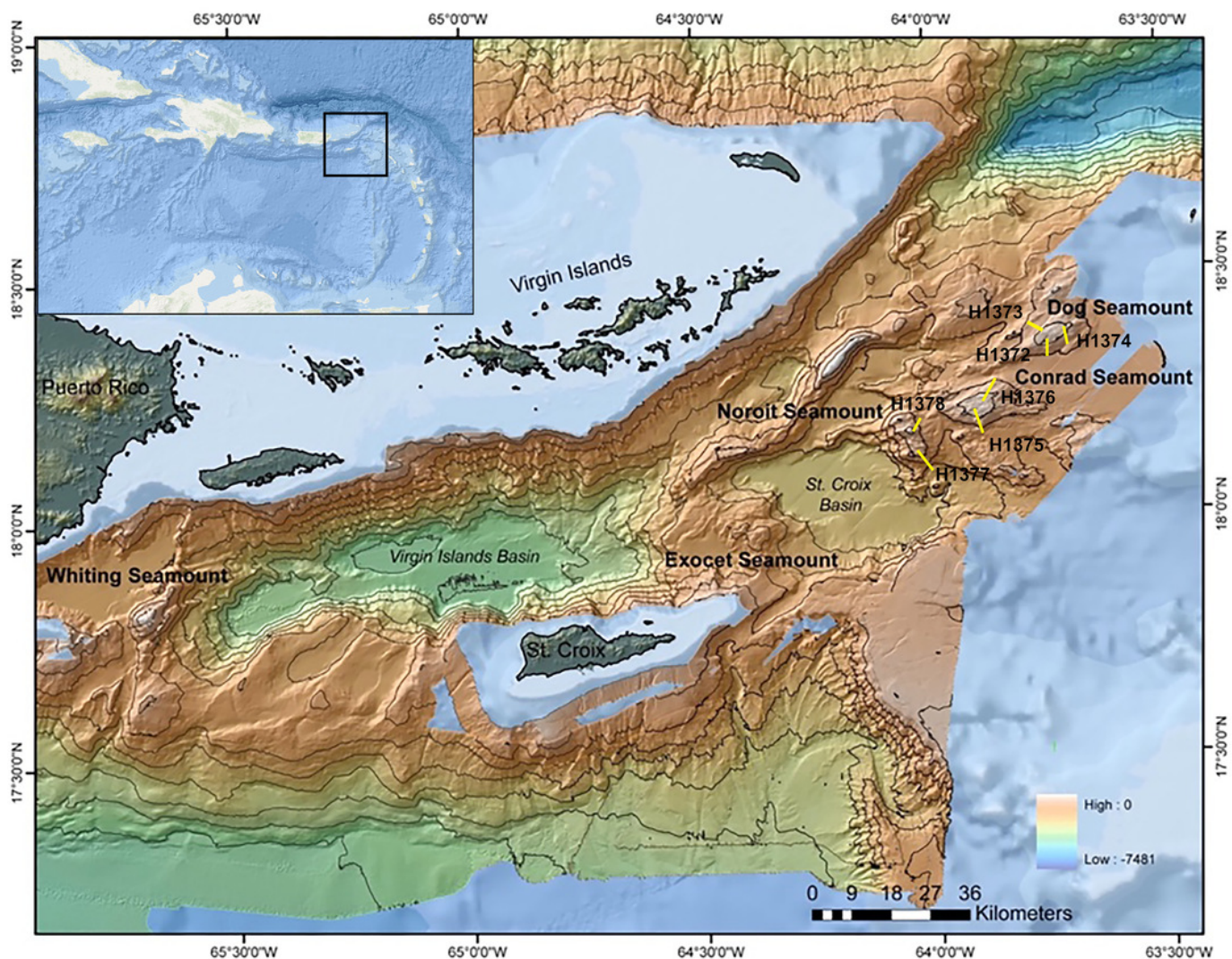
Figure 2

Temperature-Salinity plot for the Anegada Passage based on CTD water column profiles.

Water masses are overlaid and abbreviated by the following: SUW=Subtropical underwater, SSW=Sargasso Sea Water, TACW= Tropical Atlantic Central Water, AAIW=Antarctic Intermediate Water, and NADW=North Atlantic Deep Water. Isopycnal surfaces (σ_θ) are indicated in gray.
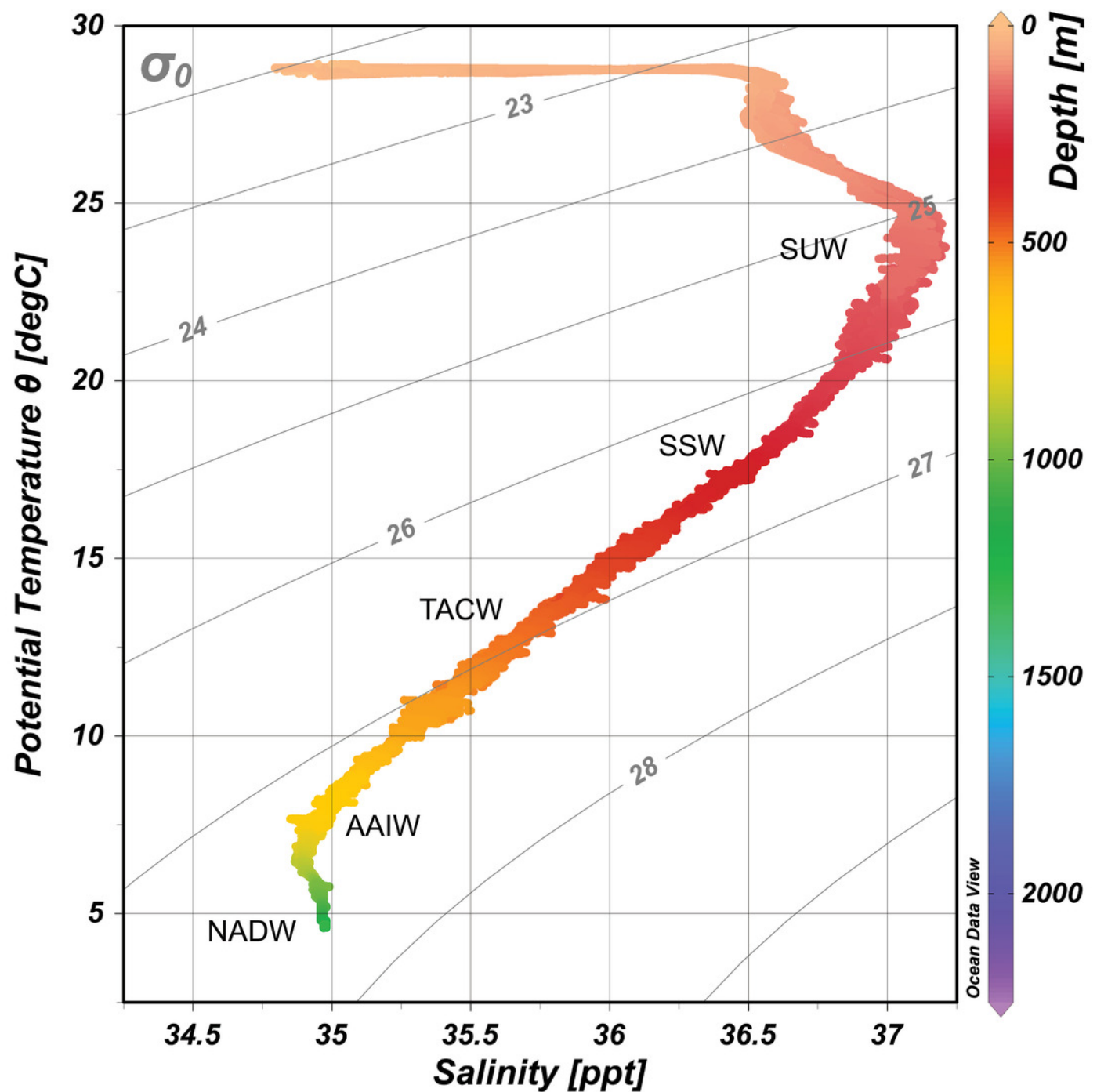
Figure 3

Depth distribution for scleractinian and stylasterid corals occurring on Dog, Conrad, and Noroît Seamounts.

Box plots represent the interquartile range with whiskers extending from the upper and lower quartiles to the minimum and maximum values. Horizontal lines represent the median depth. Individual points represent outliers. Species are arranged on the x-axis from shallowest to deepest by median depth of occurrence.
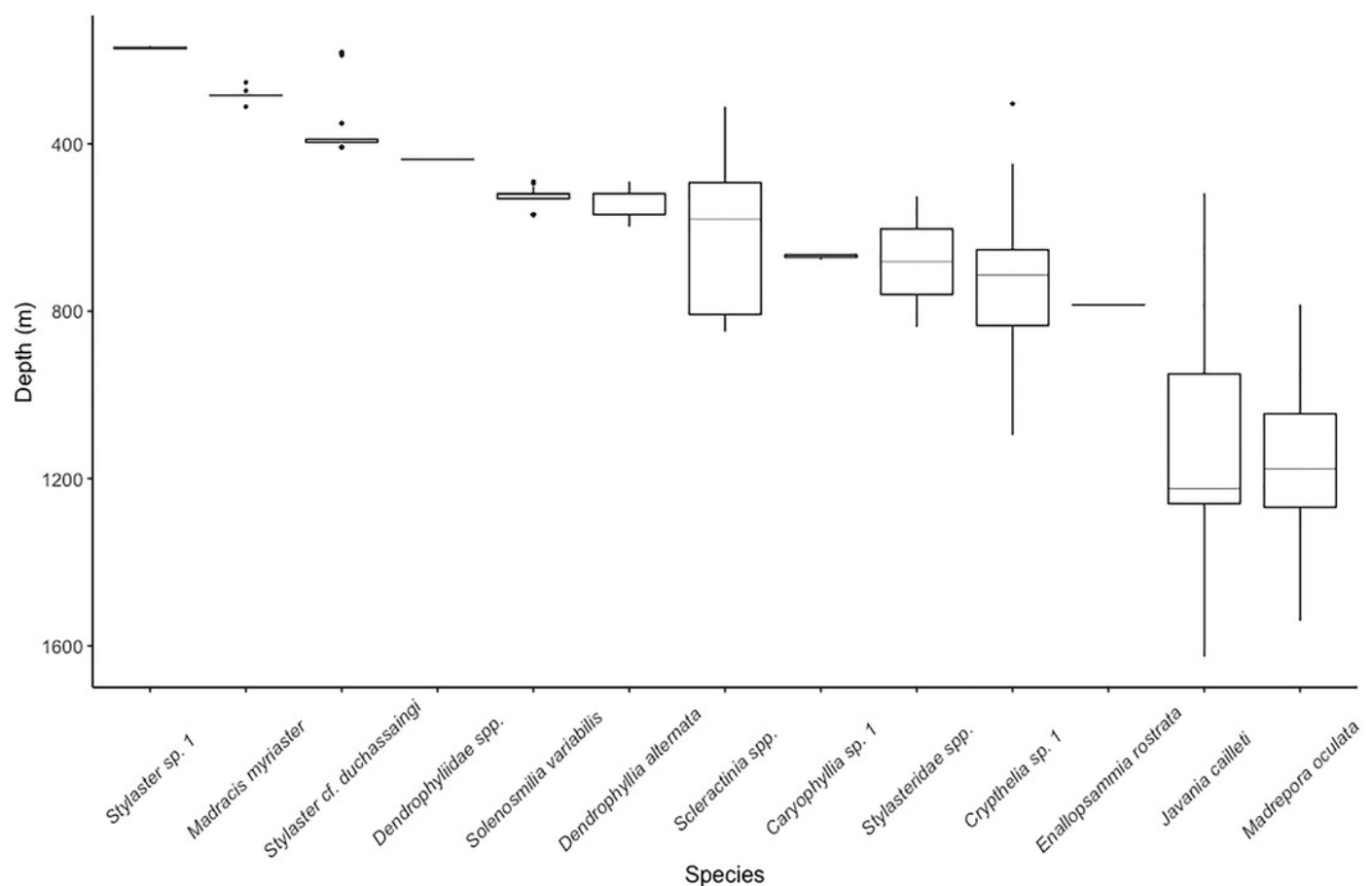
Figure 4

Distribution of scleractinian and stylasterid species against model predicted Ω_{Arag} values on the Anegada Passage seamounts.

Box plots represent the interquartile range with whiskers extending from the upper and lower quartiles to the minimum and maximum values. Vertical lines represent the median aragonite saturation state. Individual points represent outliers. Species are arranged on the y-axis from highest to lowest median aragonite saturation occurrence. A solid red vertical line indicates the aragonite saturation horizon, where $\Omega_{Arag} = 1$.
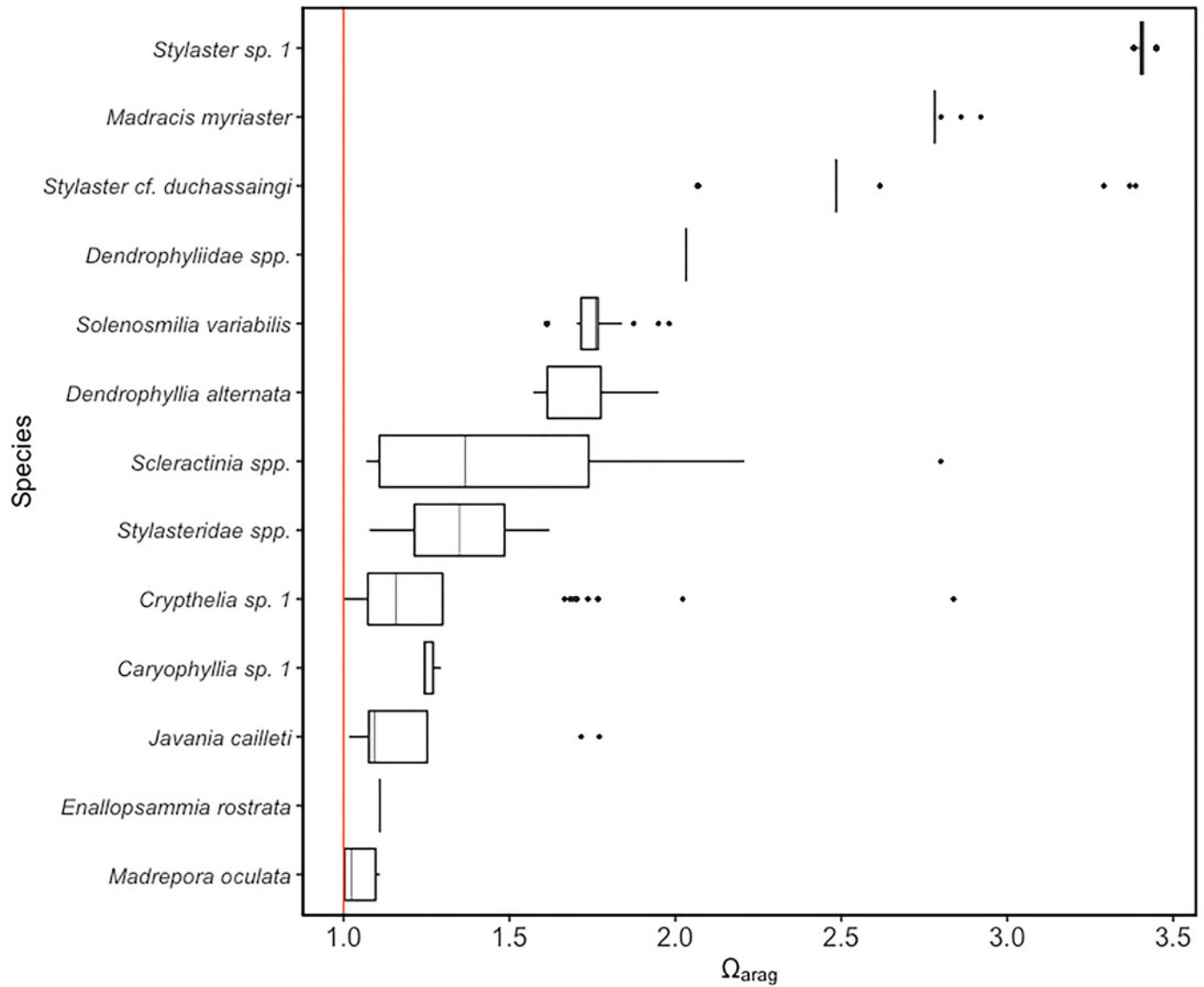
Figure 5

Species accumulation curves for the Anegada Passage seamounts.

Curves are plotted for all transects on Dog Seamount (276-1035 m), Conrad Seamount (162-1267 m), Noroit Seamount (881-2157 m), as well as for all three seamounts combined (162-2157 m).
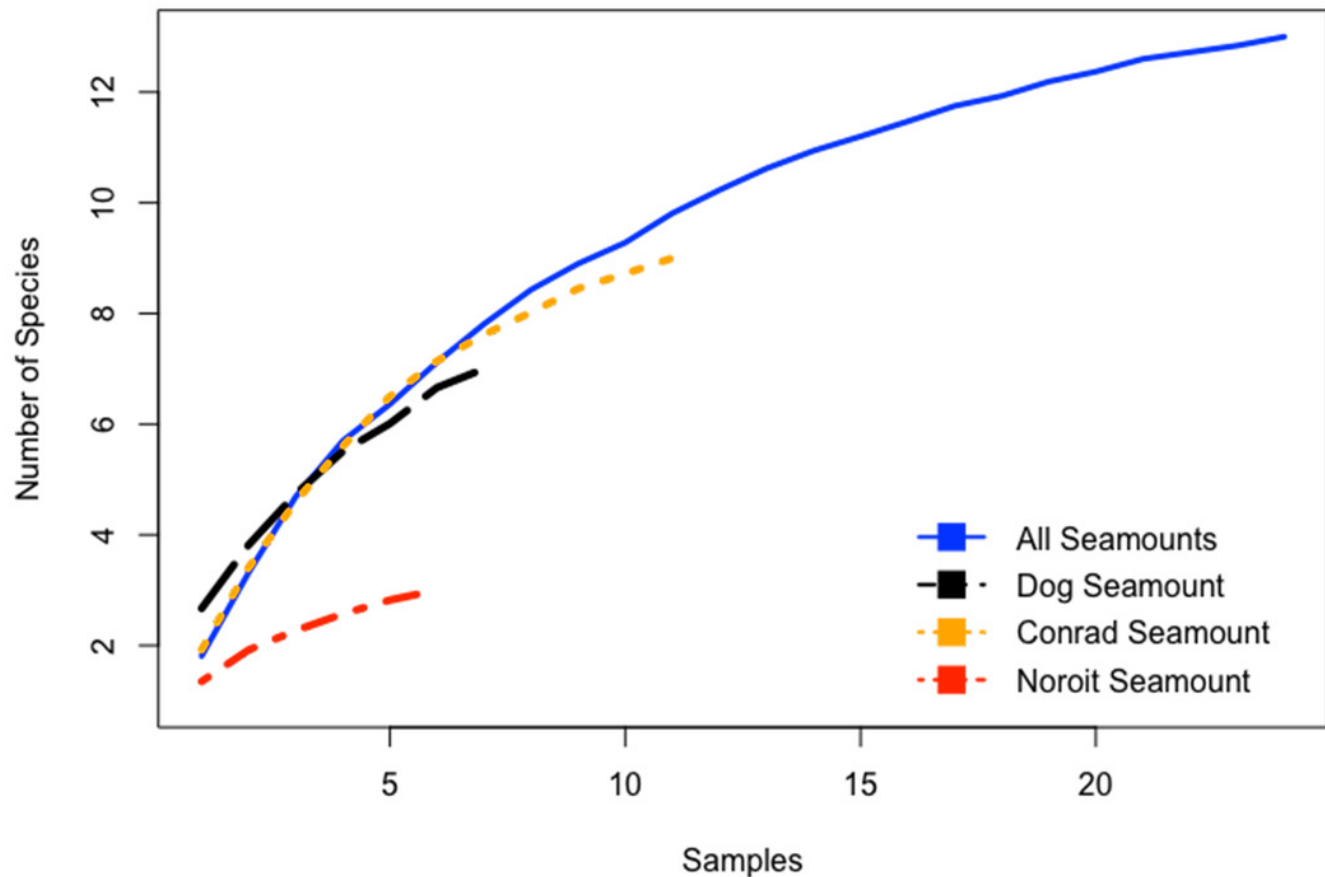
Figure 6

Non-metric multidimensional scaling analysis of standardized, fourth-root transformed coral assemblages on Dog, Conrad, and Noroît Seamounts.

SIMPROF groups are overlaid around significant groupings at the 95% level or above. Depth ranges displayed within each statistical grouping are indicated in black text. Water masses in the legend are abbreviated by the following: Subtropical underwater (SUW), Sargasso Sea Water (SSW), Tropical Atlantic Central Water (TACW), Antarctic Intermediate Water (AAIW), and North Atlantic Deep Water (NADW).
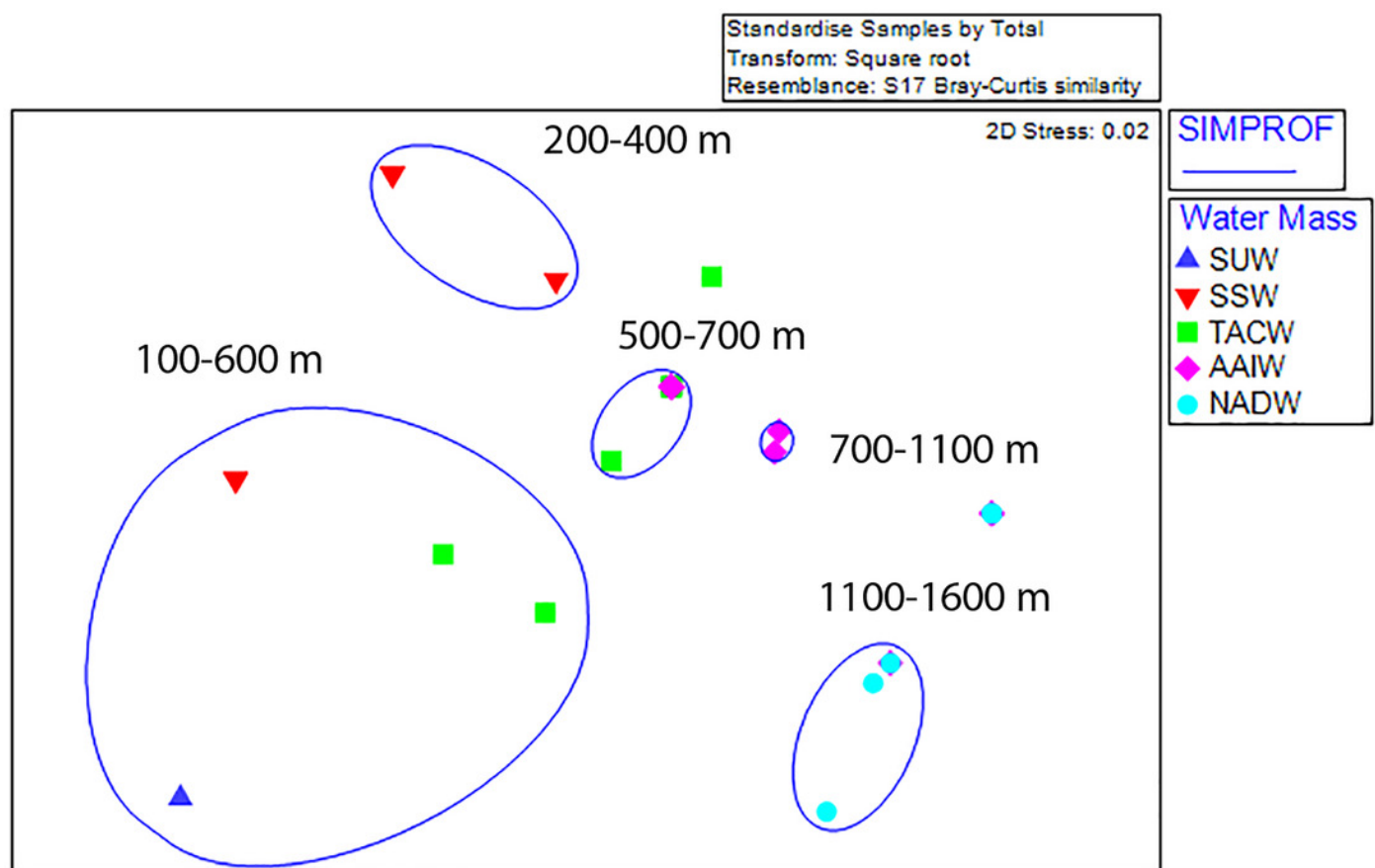
Figure 7

Distance-based linear model and redundancy analysis of coral assemblages and oceanographic variables.

Sample points represent one 100 m depth assemblage. Axes shown are the results of a distance-based redundancy analysis with percent variation explained by the first and second axes. Water masses in the legend are abbreviated by the following: Subtropical underwater (SUW), Sargasso Sea Water (SSW), Tropical Atlantic Central Water (TACW), Antarctic Intermediate Water (AAIW), and North Atlantic Deep Water (NADW).
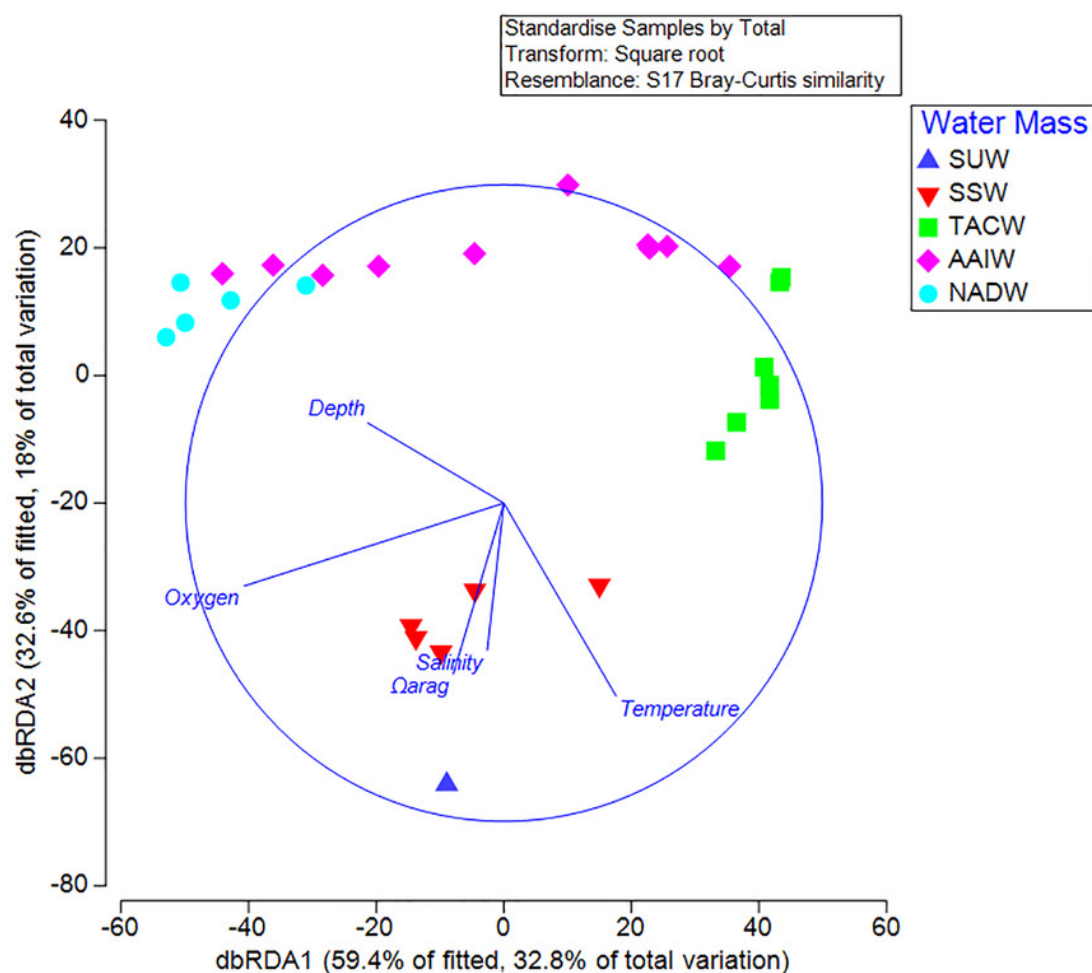
Figure 8

Deep-water scleractinians from the Anegada Passage seamounts.

(A) *Enallopsammia rostrata*. (B) *Madrepora oculata.* (C) *Madracis myriaster*. (D) *Dendrophyllia alternata.* (E) *Javania cailleti. (F) Solenosmilia variabilis*.
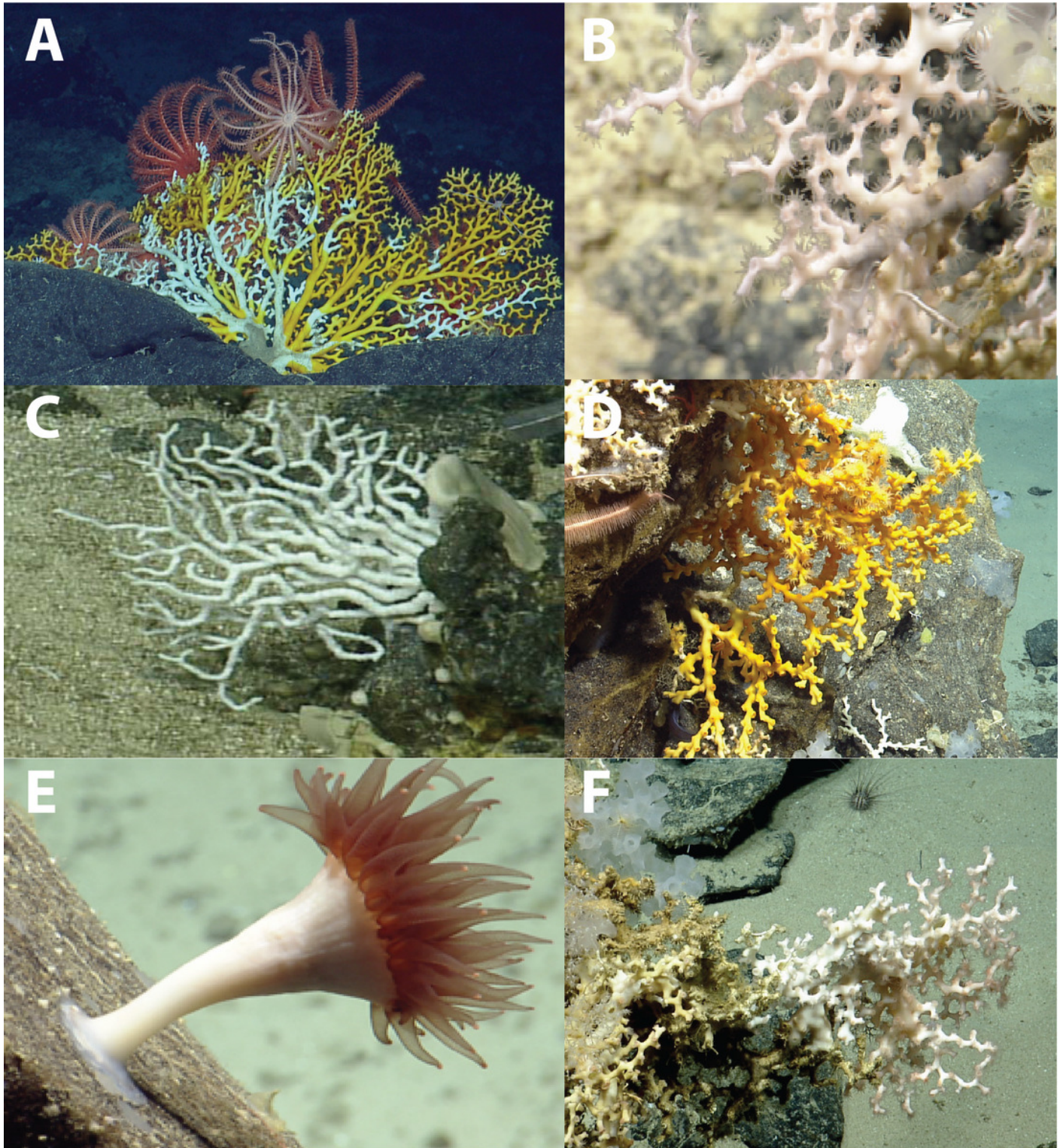
Figure 9

Deep-water stylasterids from the Anegada Passage seamounts.

(A) *Crypthelia* sp. 1. (B) *Stylaster cf. duchassaingi.* (C) *Stylaster* sp. 1.
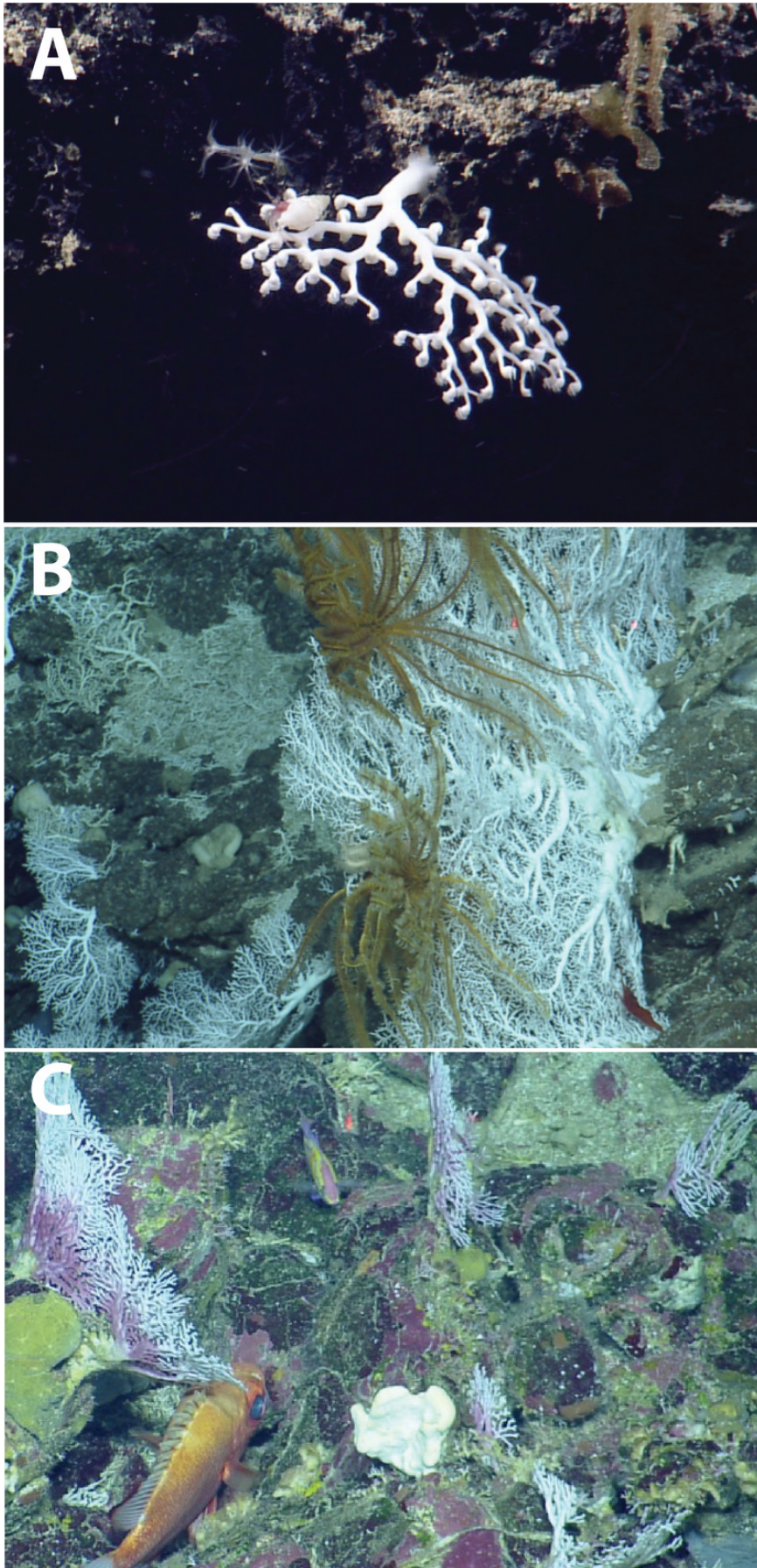
ROV dive transect details for 2014 surveys of the Anegada Passage seamounts.

Start and end coordinates for each transect, time spent in visual contact with the seafloor, and number of water samples collected at depth over the dive interval are indicated.

1   Table 1: ROV dive transect details for 2014 surveys of the Anegada Passage seamounts. Start

2   and end coordinates for each transect, time spent in visual contact with the seafloor, and number

3   of water samples collected at depth over the dive interval are indicated.

Dive	Seamount	Start Coordinates	End Coordinates	Depth Range (m)	Number of Niskin Bottle Samples	Total Bottom Time (hh:mm)
H1372	Dog	18°18.7385 N 63°46.0896 W	18°19.6177 N 63°46.1645 W	717-1035	6	07:56
H1373	Dog	18°22.6480 N 63°46.1953 W	18°21.9711 N 63°45.9306 W	503-784	6	11:09
H1374	Dog	18°20.4464 N 63°43.6091 W	18°21.9311 N 63°43.5024 W	276-601	5	09:58
H1375	Conrad	18°10.5420 N 63°53.1020 W	18°13.0029 N 63°53.3459 W	162-876	5	31:40
H1376	Conrad	18°16.4904 N 63°52.3364 W	18°14.2223 N 63°52.9767 W	344-1267	6	22:38
H1377	Noroît	18° 05.4657 N 64° 00.1741 W	18° 07.0695 N 64° 01.1760 W	881-2157	6	17:10
H1378	Noroît	18° 09.6969 N 64° 01.3606 W	18° 09.4122 N 64° 01.8888 W	949-1035	2	06:01

Summary of records and environmental variables for each taxon.

Ranges of values for number of observations, depth, temperature, salinity, dissolved oxygen, model predicted Ω_{Arag} , and colony height are reported for each species by taxonomic grouping.

1 Table 2: Summary of records and environmental variables for each taxon. Ranges of values for number of observations, depth,

2 temperature, salinity, dissolved oxygen, model predicted Ω_{Arag} , and colony height are reported for each species by taxonomic

3 grouping.

Class	Family	Species	Number of observations	Depth (m)	Temperature (°C)	Salinity (psu)	Dissolved oxygen (mg/L)	Model Predicted Ω_{arag}	Height (cm)
Hydrozoa	Stylasteridae	*Stylaster* sp. 1	65	166-174	22.1-22.5	37.00-37.05	7-7.12	3.38-3.45	-
		Crypthelia sp. 1	49	304-1096	4.9-18.0	34.53-36.55	2.41-7.22	0.99-2.83	1-12
		Stylaster cf. *duchassaingi*	30	181-408	13.8-22.1	35.82-37.01	5.39-6.99	2.07-3.39	12-37
		Stylasteridae spp.	2	525-838	6.7-10.9	34.89-35.39	4.96-5.28	1.08-1.62	3-5
Anthozoa	Caryophylliidae	*Solenosmilia variabilis*	44	490-569	10.9-13.3	35.37-35.75	4.88-5.15	1.61-1.98	12-18
		Caryophyllia sp. 1	3	665-677	8.2-8.7	35.03-35.07	4.78-4.86	1.24-1.29	-
	Oculinidae	*Madrepora oculata*	22	784-1540	4.3-6.9	34.53-34.97	5.22-8.23	1.00-1.10	10-125
	Pocilloporidae	*Madracis myriaster*	22	253-311	17.6-18.7	36.49-36.65	6.83-7.01	2.78-2.92	6-35
	Incertae familiae	Scleractinia spp. (solitary)	11	311-849	6.5-17.8	34.83-36.51	4.76-6.98	1.07-2.8	4-5
	Dendrophylliidae	*Dendrophyllia alternata*	5	490-598	10.7-13	35.33-35.71	4.84-5.13	1.57-1.95	16
		Enallopsammia rostrata	2	785	7.0	34.921	5.2	1.11	20-75
		Dendrophylliidae spp.	1	437	13.6	35.794	5.29	2.03	5
	Flabellidae	*Javania cailleti*	8	518-1626	4.2-12.0	34.557-35.54	4.96-8.34	1.02-1.77	4-7

Summary of measured values of Ω_{Arag} from water samples taken directly adjacent to corals.

Sampling events are reported for each species arranged by taxonomic grouping.

1   Table 3: Summary of measured values of Ω_{Arag} from water samples taken directly adjacent to

2   corals. Sampling events are reported for each species arranged by taxonomic grouping.

Class	Family	Species	Number of adjacent water samples	Ω_{arag} measured
Hydrozoa	Stylasteridae	*Stylaster* sp. 1	0	-
		Crypthelia sp. 1	0	-
		Stylaster cf. *duchassaingi*	0	-
		Stylasteridae spp.	0	-
Anthozoa	Caryophylliidae	*Solenosmilia variabilis*	1	1.63
		Caryophyllia sp. 1	1	1.24
	Oculinidae	*Madrepora oculata*	2	1.13-1.16
	Pocilloporidae	*Madracis myriaster*	1	2.7
	Incertae familiae	Scleractinia spp. (solitary)	0	-
	Dendrophylliidae	*Dendrophyllia alternata*	1	1.35
		Enallopsammia rostrata	1	1.21
		Dendrophylliidae spp.	1	1.82
	Flabellidae	*Javania cailleti*	1	1.16